16th World Conference on Earthquake Engineering, 16WCEE 2017

Santiago Chile, January 9th to 13th 2017

Paper N° 2283

Registration Code: S-B1463080778

WAVE PASSAGE EFFECTS ON TORSIONAL RESPONSE OF SYMMETRIC BUILDINGS IN THE NEAR-FAULT REGION

Y. Cao(1), K. C. Meza-Fajardo(2), G. P. Mavroeidis(3), A. S. Papageorgiou(4)

(1) *Graduate Student, Department of Civil and Environmental Engineering and Earth Sciences, University of Notre Dame, Notre Dame, IN 46556, USA, yenan.cao.21@nd.edu*

(2) *Researcher, BRGM, Risks and Prevention Division, Seismic and Volcanic Risks Unit, 45060 Orleans Cedex 02, France, k.mezafajardo@brgm.fr*

(3) *Assistant Professor, Department of Civil and Environmental Engineering and Earth Sciences, University of Notre Dame, Notre Dame, IN 46556, USA, g.mavroeidis@nd.edu*

(4) *Professor, Department of Civil Engineering, University of Patras, Patras 26500, Greece, papaga@upatras.gr*

Abstract

This article investigates the effects of wave passage on the torsional response of elastic buildings in the near-fault region. The model of the soil-foundation-structure system is a symmetric cylinder placed on a rigid circular foundation supported on an elastic halfspace. The idealized model is subjected to obliquely incident plane SH waves simulating the action of near-fault pulse-like motions. The response of the structure is assessed in terms of the relative twist between the top and the base of the superstructure. It is shown that the torsional response is most sensitive to a key parameter of the near-fault ground motion referred to as "pulse period". Specifically, large rotations are observed when the pulse period is close to the torsional period of the structure. It is also demonstrated that the wave passage effects are controlled by the wave apparent velocity, rather than the local site conditions. Furthermore, broadband near-fault ground motions from three hypothetical earthquakes of different magnitude are generated, and the torsional responses due to the simplified pulse-like and broadband ground motions are compared against each other. The results show that the simplified pulse model that describes the coherent seismic radiation is able to represent the main features of the near-fault ground motions that cause large torsional response. The maximum relative twist at resonance is found to be $\sim 10^{-3}$ rad, a value that is consistent with the upper bound of rotations in structures reported in the literature.

Keywords: wave passage effects; near-fault excitation; torsional response; wave apparent velocity; soil-structure interaction

1. Introduction

During an earthquake, buildings may undergo torsional response in addition to translational response. For buildings with inherent eccentricity, torsion is induced by the geometrical separation of the centers of mass and stiffness, resulting in coupled lateral-torsional response. On the other hand, spatially varying seismic excitations due to ground motion incoherence and wave passage effects contribute to the torsional response of both symmetric and asymmetric buildings.

Newmark [1] made the first rational attempt to investigate the torsional response of symmetric buildings due to base rotation arising from earthquake wave motions. Luco [2, 3] presented the mathematical formulation of the torsional steady-state response of a symmetric, elastic structure placed on a surface-supported or embedded foundation under the action of obliquely incident plane SH waves accounting for soil-structure interaction effects. It was demonstrated that large displacements associated with torsional response may be generated even for symmetric structures. De la Llera and Chopra [4] extracted base torsional excitations, associated with spatially varying ground motions, from translational ground motions recorded at the foundation level of actual buildings. It was shown that accidental torsion increases the building displacements by less than 5% for systems that are torsionally stiff or have lateral vibration periods longer than 0.5 s, whereas short period (less than 0.5 s) and torsionally flexible systems may experience a significant increase in response. Juarez and

Aviles [5] examined the combined torsional effects of structural asymmetry and foundation rotation induced by wave passage in flexibly supported structures. For a low-rise structure, the effects of foundation rotation were found to be detrimental and even more important than those of structural asymmetry, whereas the reverse was observed for a mid-rise structure.

Near-fault ground motions are frequently characterized by intense velocity and displacement pulses of relatively long duration. Even though intermediate- and long-period structures are particular susceptible to near-fault pulse-like seismic excitations, the attention regarding the effects of such motions on structures has almost exclusively focused on translational vibrations. Only a few studies have touched upon the effects of impulsive motions on the torsional response of buildings. For instance, Heredia-Zavoni and Barranco [6], although not focusing explicitly on pulse-like seismic excitations, modeled the ground motion input as a narrowband process with a dominant frequency, and concluded that torsional response due to spatially varying ground motions could be significant when the torsional period of the structure is close to the predominant period of the ground motion.

Building upon the methodology and results presented by Meza-Fajardo [7] (see also Meza-Fajardo and Papageorgiou [8]), this article aims to identify the key parameters of the soil-foundation-structure system and ground motion input that control the effects of wave passage on the torsional response of symmetric, elastic buildings under the action of near-fault pulse-like motions. The soil-foundation-structure model proposed by Luco [2] is adopted to calculate the torsional response of the buildings, whereas the mathematical model proposed by Mavroeidis and Papageorgiou [9] is used to describe the coherent component of the near-fault ground motions. The torsional response is investigated through a detailed parametric analysis using realistic physical properties of the soil-foundation-structure system. Finally, the torsional response due to simplified and broadband ground motions are compared to assess the effectiveness of idealized pulse models to estimate accurately the building torsional response due to wave passage in the near-fault region. It should be noted that detailed results pertaining to this study are presented by Cao et al. [10].

2. Soil-Foundation-Structure System

2.1 Model configuration

Fig. 1 illustrates the soil-foundation-structure model under the action of an obliquely incident plane SH wave proposed by Luco [2]. The superstructure is modeled by a uniform elastic bar of height H and radius a with mass moment of inertial about the z-axis I_{b}, hysteretic damping factor ξ, and fixed-base fundamental frequency in torsion ω_1. The foundation is represented by a rigid circular disc with the same radius as that of the superstructure and mass moment of inertia with respect to the z-axis I_0. The soil is assumed to be an elastic, homogeneous and isotropic halfspace with density ρ_s, shear modulus μ, and shear wave velocity β. The plane SH wave is assumed to propagate at an angle Θ with respect to the x axis and the particle movement is parallel to the y axis.

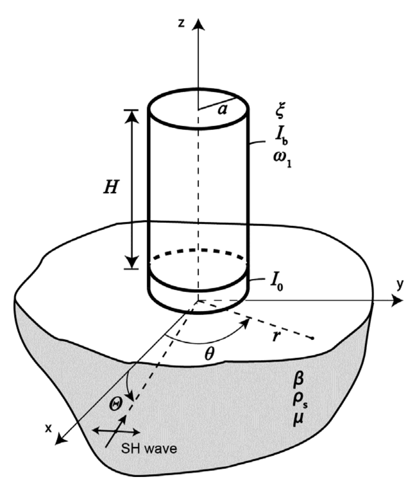

Fig. 1 – Model of the soil-foundation-structure system (modified after Luco [2]).

2.2 Transfer function

The torsional response in the frequency domain (also known as transfer function) of the soil-foundation-structure system has been derived analytically by Luco [2] and is briefly presented in this section. The average value of the tangential component of displacement $\bar{u}_\theta$ of the rigid circular foundation is decomposed into three parts:

$$\bar{u}_\theta = \bar{u}_\theta^{i+r} + \bar{u}_\theta^{R} + \bar{u}_\theta^{S} \tag{1}$$

where $\bar{u}_\theta^{i+r}$ is the average tangential component of the free-field ground motion, $\bar{u}_\theta^{R}$ is the motion generated by the foundation twist in the absence of seismic excitation, and $\bar{u}_\theta^{S}$ is the average tangential component of motion that needs to be added to the free-field motion when the foundation is kept fixed under the action of seismic excitation. Once the average tangential displacement field $\bar{u}_\theta$ is obtained, the average tangential stress field $\bar{\sigma}_{z\theta}$ may be evaluated by

$$\bar{\sigma}_{z\theta}\,(r,z) = \frac{1}{2\pi}\int_0^{2\pi} \sigma_{z\theta}\,(r,\theta,z)\,d\theta = \mu\frac{\partial \bar{u}_\theta}{\partial z} \tag{2}$$

The total torque $T_s e^{i\omega t}$ that the rigid foundation exerts on the soil can then be calculated by integrating the average tangential stress field $\bar{\sigma}_{z\theta}$ along the radius a and by setting z=0:

$$T_s e^{i\omega t} = 2\pi \int_0^{a} \bar{\sigma}_{z\theta}\,(r,0) r^2\, dr \tag{3}$$

By combining Eqs. (1)-(3) and after lengthy derivations, T_s can be expressed by

$$T_s = K_{\mathrm{TT}}(a_0)(\alpha_{\mathrm{b}} - \alpha^*) \tag{4}$$

where $K_{\mathrm{TT}}(a_0)$ is the torsional impedance function for the foundation calculated as

$$K_{\mathrm{TT}}(a_0) = 16\mu a^3 \int_0^1 t\theta_{\mathrm{R}}(t)dt\,; \qquad a_0 = a\omega/\beta \tag{5}$$

α_{b} is the twist angle of the foundation (also known as base twist), and α^* is the input twist that corresponds to the rotation of the rigid foundation under the action of seismic excitation when no external forces are acting on the foundation ($T_s = 0$):

$$\alpha^* = \left(8i\mu a^3 a_0 \cos\Theta \int_0^1 t\theta_{\mathrm{s}}(t)dt \,/ K_{\mathrm{TT}}(a_0)\right) u_{\mathrm{g0}}/a \tag{6}$$

By considering the torque-twist relationship for the superstructure and the coupling of superstructure and soil through the foundation, the base twist α_{b} can be expressed as

$$\frac{a\alpha_{\mathrm{b}}(\omega)}{u_{\mathrm{g0}}} = \frac{S\left(a_1\dfrac{\omega}{\omega_1},\Theta\right)}{1-\dfrac{\pi}{20}\left(a_1\dfrac{\omega}{\omega_1}\right)^2\left\{\dfrac{I_0}{I_{\mathrm{s}}}+\dfrac{I_{\mathrm{b}}}{I_{\mathrm{s}}}\left[\dfrac{\tan\left[\dfrac{\pi}{2}\left(\dfrac{\omega}{\omega_1}\right)\dfrac{1}{\sqrt{1+2i\xi}}\right]}{\dfrac{\pi}{2}\left(\dfrac{\omega}{\omega_1}\right)\dfrac{1}{\sqrt{1+2i\xi}}}\right]\right\}\dfrac{K_{\mathrm{TT}}(0)}{K_{\mathrm{TT}}\left(a_1\dfrac{\omega}{\omega_1}\right)}} \tag{7}$$

where

$$S\left(a_1\frac{\omega}{\omega_1},\Theta\right) = a\,\alpha^*/\,u_{\mathrm{g0}}, \quad a_1 = a\omega_1/\beta = a_0\omega_1/\omega,$$
$$I_{\mathrm{s}} = \tfrac{4\pi}{15}\rho_{\mathrm{s}}a^5, \quad I_{\mathrm{b}} = \tfrac{1}{2}m_{\mathrm{b}}a^2, \quad I_0 = \tfrac{1}{2}m_0 a^2 \tag{8a-e}$$

with m_{b} and m_0 denoting the masses of the superstructure and the foundation, respectively. The twist at the top of the superstructure α_{t} can then be expressed as a function of the base twist α_{b} by

$$\alpha_{\mathrm{t}}(\omega) = \alpha_{\mathrm{b}}(\omega)\sec\left[\frac{\pi}{2}\left(\frac{\omega}{\omega_1}\right)\frac{1}{\sqrt{1+2i\xi}}\right] \tag{9}$$

whereas the relative twist between the top and the base of the superstructure α_{r} can be defined as

$$\alpha_{\mathrm{r}}(\omega) = \alpha_{\mathrm{t}}(\omega) - \alpha_{\mathrm{b}}(\omega) \tag{10}$$

In summary, the transfer function of the relative twist of the soil-foundation-structure system may be described in terms of the following dimensionless parameters: normalized frequency ω/ω_1, stiffness of the superstructure relative to that of the soil a_1 (also known as relative stiffness parameter), ratios of moments of inertia $I_{\mathrm{b}}/I_{\mathrm{s}}$ and I_0/I_{s}, hysteretic damping factor ξ, and angle of incidence Θ.

2.3 Input parameters

Table 1 summarizes the basic characteristics of the 40 buildings considered in this study along with their site conditions. This information has been obtained from the empirical evaluation of soil-structure interaction effects conducted by Stewart et al. [11, 12]. The foundation radius adopted herein is the radius of a circular disc whose area matches the area of the actual foundation [12]. Consistent with findings of previous studies on the evaluation of vibration properties of buildings (e.g. [13]), the torsional fundamental period T_1 is assumed to be equal to 80% of the fixed-base translational period of the fundamental mode. The relative stiffness parameter a_1 for each building listed in Table 1 can be calculated by substituting the radius a, the torsional fundamental frequency $\omega_1 = 2\pi/T_1$, and the shear wave velocity β in Eq. (8b). The majority of the 40 buildings have a_1 values between 0.1 and 1.75, whereas a few stiff buildings (occasionally with large radius) on soft soil conditions (i.e. small shear wave velocity) are characterized by values of a_1 between 2.0 and 5.5. The ratios of moments of inertia, $I_{\mathrm{b}}/I_{\mathrm{s}}$ and I_0/I_{s}, can be calculated by using Eq. (8c-e) in conjunction with the foundation radius a and typical values of ρ_{s}, m_{b} and m_0. For instance, the soil density ρ_{s} ranges from 1.5-2.4 $\mathrm{Mg/m^3}$ depending on the type of soil. The mass of the superstructure m_{b} for typical residential and office buildings may be calculated as follows:

$$m_{\mathrm{b}} = \rho_{\mathrm{b}}\, H\, A \tag{11a}$$

with

$$\rho_{\mathrm{b}} \approx \frac{q}{g h_0} \tag{11b}$$

where ρ_{b} is the mass density of the superstructure, H and $A = \pi a^2$ are the height and floor area of the building, h_0 is the interstory height, and q is the gravity load consisting of dead and live loads. Once the mass of the superstructure m_{b} has been calculated using Eq. (11), the mass of the foundation m_0 can be estimated for typical buildings (e.g. [5, 14]) as:

$$m_0 \approx (0.05 - 0.35)m_{\mathrm{b}} \tag{12}$$

The interstory height for residential and office buildings is about 3.5 m (11.5 ft). Average gross dead loads are 4.8-7.2 $\mathrm{kN/m^2}$ (100-150 $\mathrm{lb/ft^2}$) for reinforced concrete buildings and 2.9-3.8 $\mathrm{kN/m^2}$ (60-80 $\mathrm{lb/ft^2}$) for steel framed buildings, whereas the minimum uniformly distributed live loads typically vary between 1.9-4.8 $\mathrm{kN/m^2}$ (40-100 $\mathrm{lb/ft^2}$) depending on the occupancy characterization of the building [15]. By considering the aforementioned values of interstory height, dead load and live load, the mass density of the superstructure ρ_{b} of Eq. (11b) is estimated in the range of 150-350 $\mathrm{kg/m^3}$.

Representative values of $I_{\mathrm{b}}/I_{\mathrm{s}}$ can be calculated by combining Eqs. (8c,d) and (11) and by setting ρ_{s} and ρ_{b} equal to their average values (i.e. ρ_{s} = 1.95 $\mathrm{Mg/m^3}$, ρ_{b} = 250 $\mathrm{kg/m^3}$). For the buildings listed in Table 1, the majority of the $I_{\mathrm{b}}/I_{\mathrm{s}}$ values are between 0.1 and 0.7. Buildings with $I_{\mathrm{b}}/I_{\mathrm{s}}$ > 0.7 are typically characterized by large H/a ratios. Provided that the superstructure and the foundation have the same radius a, the ratio of I_0/I_{s} can be calculated by multiplying $I_{\mathrm{b}}/I_{\mathrm{s}}$ with the foundation-to-superstructure mass ratio m_0/m_{b}, which has been shown to vary between 0.05 and 0.35 according to Eq. (12).

The hysteretic damping factor ξ is approximated by the equivalent viscous damping ratio. In general, viscous damping ratios are spread over a relatively wide range (0.5-9.0%) depending on the material and height of the building. Estimates of viscous damping ratios are also sensitive to the system identification algorithm utilized in the analysis, as well as the type and level of excitation used as an input. For buildings subjected to earthquake loads, values of ξ = 3% and 5% are typically assumed for steel and concrete buildings, respectively.

For the results presented in this study, the soil density ρ_s, the mass density of the superstructure ρ_b, the foundation-to-superstructure mass ratio m_0/m_b, and the hysteretic damping factor ξ are set equal to their average values (i.e. ρ_s = 1.95 $\mathrm{Mg/m^3}$, ρ_b = 250 $\mathrm{kg/m^3}$, m_0/m_b = 0.2, and ξ = 4%).

Table 1 – Buildings considered in present study (modified after Stewart et al. [11, 12])

Site index[a]	Building	Structural system[b]	No. stories	Height[c] (m)	Foundation radius[d] (m)	Fixed-base fundamental translational period (s)	Soil shear wave velocity (m/s)
“A” Sites							
1	Eureka Silvercrest Apts.	SW	5	13.5	17.4	0.15	213.7
4	Emeryville Pacific Pk. Plaza	CF	31	94.9	26.5	2.45	136.6
5	Hayward City Hall	DWF	11	36.6	20.1	1.11	673.6
8	Piedmont Jr. High School	SW	3	10.9	15.8	0.16	554.7
10	Richmond City Hall	DWF	3	14.4	22.9	0.28	234.1
11	San Jose 3-St. Offc. Bldg.	SF	3	15.2	26.2	0.67	805.3
12	El Centro Imp. Co. Ser. Bldg.	DWF	6	23.5	18.6	0.50	141.4
13	Indio 4-St. Gov’t Offc. Bldg.	DWF	4	24.4	21.0	0.67	211.8
14	Lancaster 3-St. Offc. Bldg.	SW	3	11.3	16.5	0.20	276.8
15	Lancaster 5-St. Hospital	SF	5	17.4	30.2	0.69	305.1
17	Loma Linda VA Hos.	SW	4	21.8	75.0	0.25	431.3
20	Long Beach VA Hospital	SW	11	42.7	25.6	0.51	348.4
23	LA 6-St. Offc. Bldg.	SF	5	24.4	6.5	0.82	192.0
24	LA 6-St. Pkg. Garage	SW	6	17.4	48.5	0.51	265.2
26	LA 7-St. UCLA Bldg.	DWF	7	28.7	10.1	0.63	167.0
27	LA 15-St. Offc. Bldg.	SF	17	75.8	39.9	3.20	353.9
28	LA 19-St. Offc. Bldg.	SF	19	95.8	28.0	3.45	298.7
29	LA Hollywood Storage Bldg.	CF	14	41.8	18.0	1.77	283.5
30	LA Wadsworth VA Hospital	SF	6	34.0	57.6	0.92	299.0
31	Newport Beach Hoag Hospital	SW	11	40.9	18.6	0.70	307.5
33	Norwalk 12440 Imp. Hwy.	SF	7	31.4	43.3	1.30	276.2
34	Palmdale 4-St. Hotel	SW	4	10.5	21.0	0.12	480.1
35	Pomona 2-St. Bldg.	CF	2	12.2	18.0	0.25	379.8
36	Pomona 6-St. Bldg.	CF	6	23.1	15.2	1.07	362.1
38	San Bernardino 3-St.	SF	3	12.6	23.8	0.52	269.1
39	San Bernardino 5-St.	SW	5	22.6	29.0	0.65	375.8
40	San Bernardino Vanir Tower	SF	9	32.2	16.8	2.01	258.5
41	San Bernardino Co. Govt Cntr	SF	5	16.5	34.7	0.51	308.2
44	Sylmar Olive View Med. Cen	SW	6	27.4	38.4	0.27	459.0
45	Ventura 12-St. Hotel	SW	12	30.0	18.9	0.53	270.1
“B” Sites							
2	San Bruno 9-St. Offc. Bldg.	SW	9	28.7	21.9	0.97	279.2
3	San Fran. 47-St. Offc. Bldg.	SF	47	180.3	26.2	5.03	145.7
5	San Jose 10-St. Resid. Bldg.	SW	10	26.6	19.8	0.29	234.1
6	San Jose 13-St. Gov’t Offc.	SF	12	47.5	25.3	2.13	221.0
7	Walnut Creek 10-St. Offc.	DWF	10	38.8	9.8	0.66	428.2
10	LA 9-St. Offc. Bldg.	DWF	9	38.8	15.2	1.25	267.6
11	LA 17-St. Resid. Bldg.	SW	17	39.6	23.2	0.85	362.7
12	LA 32-St. Offc. Bldg.	DWF	32	130.6	28.3	1.84	408.1
13	LA 54-St. Offc. Bldg.	SF	54	180.3	29.3	5.70	401.4
14	Whittier 8-St. Hotel	SW	8	20.9	19.5	0.49	256.6

[a] Site classes “A” and “B” correspond to sites with or without a free-field accelerograph in the system identification study conducted by Stewart et al. [12].

[b] Lateral force resisting system: SW=masonry or concrete shear wall, DWF=dual wall/frame, CF=concrete frame, SF=steel frame.

[c] Full height of structure derived from the effective height reported by Stewart et al. [12] (i.e. effective height = 0.7 * full height).

[d] Foundation radius matching the area of the actual foundation.

3. Near-Fault Ground Motions

3.1 Mathematical model

The mathematical model proposed by Mavroeidis and Papageorgiou [9] is adopted to describe the coherent component of the seismic excitation input in the near-fault region. The mathematical formulation for the representation of the near-fault velocity pulses is the product of a harmonic oscillation and a bell-shaped function, that is:

$$v(t) = \begin{cases} \frac{A}{2}\left[1+\cos\left(\frac{2\pi f_\mathrm{P}}{\gamma}(t-t_0)\right)\right]\cos[2\pi f_\mathrm{P}(t-t_0)+\nu], & t_0-\frac{\gamma}{2f_\mathrm{P}} \le t \le t_0+\frac{\gamma}{2f_\mathrm{P}} \text{ with } \gamma > 1 \\ 0, & \text{otherwise} \end{cases} \tag{13}$$

where A controls the amplitude of the signal, f_P is the prevailing frequency of the signal, ν is the phase of the amplitude-modulated harmonic, γ is a parameter that defines the oscillatory character of the signal, and t_0 specifies the epoch of the envelope's peak. The pulse period T_P is defined as the inverse of the prevailing frequency f_P, thus providing an "objective" assessment of this important parameter:

$$T_\mathrm{P} = \frac{1}{f_\mathrm{P}} \tag{14}$$

Mavroeidis and Papageorgiou [9] also derived a closed-form expression for the Fourier transform $V(\omega)$ of the velocity signal provided by Eq. (13) as a function of A, T_P, γ, and ν. The Fourier transform $D(\omega)$ of the corresponding displacement signal can readily be derived by the following equation:

$$D(\omega) = \frac{V(\omega)}{\mathrm{i}\omega} \tag{15}$$

3.2 Input parameters

In previous studies, the scaling characteristics of the model input parameters were investigated using a large set of actual near-fault ground motion records affected by forward directivity, and simple empirical relationships were proposed. Mavroeidis and Papageorgiou [9] obtained the following relationship between the pulse period T_P and the earthquake magnitude M_W:

$$\log T_\mathrm{P} = -2.9 + 0.5 M_\mathrm{W} \tag{16}$$

The amplitude of the near-fault velocity records appears to be a fairly stable parameter. A value of 100 cm/s effectively represents peak ground velocities within a few kilometers from the causative fault regardless of the earthquake magnitude [9]. Finally, parameter γ varies from a value slightly larger than 1 up to a maximum value of 3, whereas the phase angle ν varies from 0 to 360$^\mathrm{o}$.

In this study, T_P ranges from 0.5 to 10 s with an increment of 0.05 s. According to Eq. (16), this range of values for T_P corresponds to earthquake magnitudes M_W between 5.2 and 7.8. Parameter A is fixed to 100 cm/s based on the recommendation made by Mavroeidis and Papageorgiou [9] and Mavroeidis et al. [16] for sites located within a few kilometers from the causative fault. The effect of γ is taken into account by considering four characteristic values: 1.0, 1.5, 2.0, and 3.0. Finally, parameter ν is set equal to 90$^\mathrm{o}$ to ensure that the displacement offset vanishes for all generated motions in agreement with the waveform characteristics of pure forward directivity motions.

4. Torsional Response due to Simplified Near-Fault Pulse-Like Ground Motions

The torsional response of the soil-foundation-structure system in the frequency domain is first calculated by multiplying the transfer function of the relative twist $\alpha_\mathrm{r}(\omega)$ of the superstructure with the Fourier transform $D(\omega)$ of the simplified ground displacement. The relative twist of the superstructure in the time domain is then obtained by applying the inverse Fast Fourier transform. The response quantity of interest is the maximum relative twist expressed in radians.

4.1 Effect of ground motion parameters

Three buildings with short, intermediate and long periods are selected from Table 1 to examine the effect of ground motion parameters on torsional response: Building A10 (3 stories, $H = 14.4$ m, $a = 22.9$ m, $T_1 = 0.22$ s and $\beta = 234.1$ m/s), Building A36 (6 stories, $H = 23.1$ m, $a = 15.2$ m, $T_1 = 0.86$ s and $\beta = 362.1$ m/s), and Building A28 (19 stories, $H = 95.8$ m, $a = 28.0$ m, $T_1 = 2.76$ s and $\beta = 298.7$ m/s). Fig. 2 presents the maximum relative twist of the three buildings as a function of the normalized period T_P/T_1 for different values of γ and Θ. Since the T_P values considered in this study range from 0.5 to 10 s (corresponding to M_W 5.2-7.8), the effective range of T_P/T_1 over which Fig. 2 is plotted differs for each of the three buildings because of their distinct torsional periods T_1. With reference to Fig. 2, the following observations are made:

- The global peak of the maximum relative twist is attained when $T_\mathrm{P}/\mathrm{T}_1$ approaches a value slightly larger than one (see Buildings A28 and A36), indicating that resonance occurs when the pulse period approaches the torsional period of the building. Building A10 is not subjected to resonance response due to the range of $T_\mathrm{P}/\mathrm{T}_1$ values considered in this study, and thus the response tends to be significantly smaller than the response of Buildings A28 and A36.
- As γ increases from 1 to 3, the global peak of the maximum relative twist (resonance response) increases by a factor of ~2 and the shape of the response curve changes gradually from "flattened" to "peaked". It is also worth mentioning that for $T_\mathrm{P}/T_1 > 1.5$, the maximum relative twist decreases as γ increases from 1 to 3.
- Comparison of Figs. 2a and b indicates that the maximum relative twist decreases significantly as Θ increases from 40° to 80°.
- The maximum relative twists for the short-, intermediate- and long-period buildings shown in Figs. 2a or b cannot be compared to one another in a meaningful way, even for fixed values of γ and Θ. In addition to γ and Θ, the maximum relative twist depends on various parameters, including a, $I_\mathrm{b}/I_\mathrm{s}$, a_1 (which also incorporates the effect of β), as well as ω_P (or equivalently T_P) and ω_1 (or equivalently T_1).

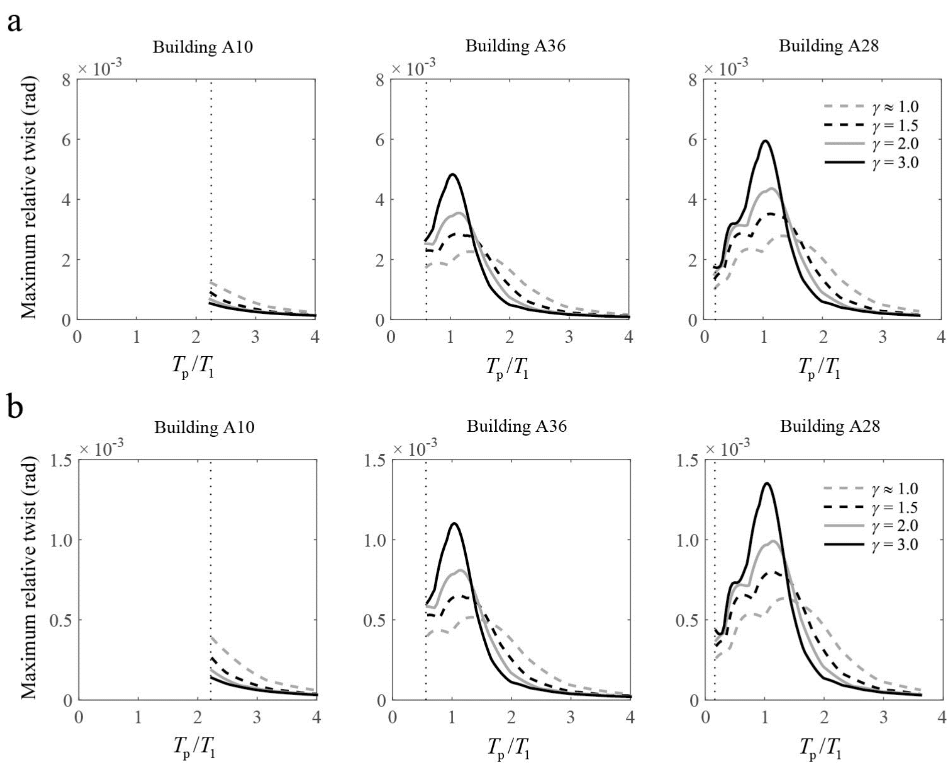

Fig. 2 – Maximum relative twist between top and base of Buildings A10, A36 and A28 vs. T_P/T_1 for $\gamma = 1.0, 1.5, 2.0, 3.0$. The angle of incidence is considered to be Θ = 40° and 80° for (a) and (b), respectively. The dotted vertical line specifies the lower limit of the effective range of T_P/T_1 for each building.

4.2 Physical constraints on angle of incidence

As was shown in Section 4.1, the maximum relative twist depends on the angle of incidence Θ. In reality, the impinging directions of the traveling seismic waves are considerably close to vertical. The primary reason is that soils are layered with shear wave velocities increasing with depth and therefore the refractions of waves at the layer interfaces cause the waves to travel in a more vertical direction as they approach the ground surface (e.g. [17]).

The angle of incidence Θ of a plane SH wave and the shear wave velocity β at the top soil layer are related through the following equation:

$$c_{\mathrm{H}} = \frac{\beta}{\cos\Theta} \tag{17}$$

where c_{H} is the wave apparent horizontal velocity. Previous studies published in the literature have estimated the range of c_{H} values of body waves in the near-fault region using empirical or numerical approaches. For instance, O'Rourke et al. [17] approximated c_{H} at a particular site based on the three acceleration components of ground motion and the material properties of the top layer. The method was applied to several sites that recorded the 1971 San Fernando and 1979 Imperial Valley earthquakes, and the median c_{H} values reported by O'Rourke et al. [17] for the two earthquakes were 2.1 and 3.8 $\mathrm{km/s}$, respectively. Through numerical simulations of ground motion in the near-fault region, Bouchon and Aki [18] concluded that c_{H} is controlled by the rupture velocity on the fault plane or the shear wave velocity of the basement rock with values ranging between 2.2 and 3.5 $\mathrm{km/s}$.

Three representative values of c_{H} (i.e. 2.0, 2.9 and 3.8 $\mathrm{km/s}$) and four representative values of β (i.e. 1130, 560, 270 and 170 $\mathrm{m/s}$) corresponding to the National Earthquake Hazards Reduction Program (NEHRP) Site Classes B, C, D and E are selected. By substituting these representative c_{H} and β values into Eq. (17), the angle of incidence Θ is estimated to vary between 55.6° and 87.4°, suggesting that the impinging directions of the traveling seismic waves are mostly close to vertical. Note that the adopted values of β aim to examine the effect of different soil types on torsional response and do not necessarily reflect the site conditions of any particular building listed in Table 1.

Fig. 3 illustrates the maximum relative twist of the three buildings shown in Fig. 2 (Buildings A10, A28 and A36) as a function of the normalized period T_{P}/T_1 for $\gamma = 2.0$ and distinct values of $c_{\mathrm{H}} = 2.0, 2.9, 3.8\ \mathrm{km/s}$ and $\beta = 170, 270, 560, 1130\ \mathrm{m/s}$. Each line style represents a certain wave apparent velocity, whereas the four shear wave velocities are not specified individually since their impact on the torsional response for a particular c_{H} value is insignificant. Fig. 3 shows that the maximum relative twist increases as c_{H} decreases. This observation is consistent with findings reported in the literature indicating that a lower value of c_{H} would induce a larger torsional response (e.g. [19, 20]). More importantly, Fig. 3 suggests that it is the wave apparent velocity c_{H} rather than the local site condition that determines the relative torsional response of the superstructure.

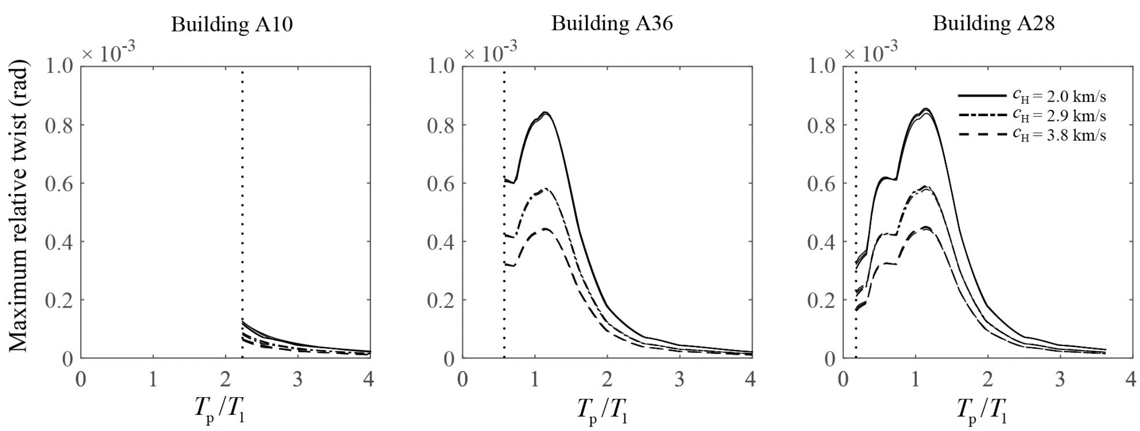

Fig. 3 – Maximum relative twist between top and base of Buildings A10, A36 and A28 vs. T_{P}/T_1 for $c_{\mathrm{H}} = 2.0, 2.9, 3.8\ \mathrm{km/s}$ and $\beta = 170, 270, 560, 1130\ \mathrm{m/s}$. Parameter γ is set equal to 2.0.

4.3 Effect of building parameters

Fig. 4 presents the maximum relative twist of all 40 buildings listed in Table 1 as a function of T_{P}/T_1 for $\beta = 170, 270, 560, 1130\ \mathrm{m/s}$ and $\gamma = 2.0$, whereas c_{H} is selected as 2.0 km/s to obtain the most critical response. Note that the effective range of T_{P}/T_1 over which each response curve is plotted is different for each building because of its distinct torsional period T_1. Fig. 4 shows that both the shape and amplitude of the response curves are remarkably similar to one another, especially as the shear wave velocity increases. The result indicates that building parameters such as height and radius have a relatively insignificant effect on the torsional response, especially for stiff soil conditions, whereas the period ratio T_{P}/T_1 is clearly the dominant parameter.

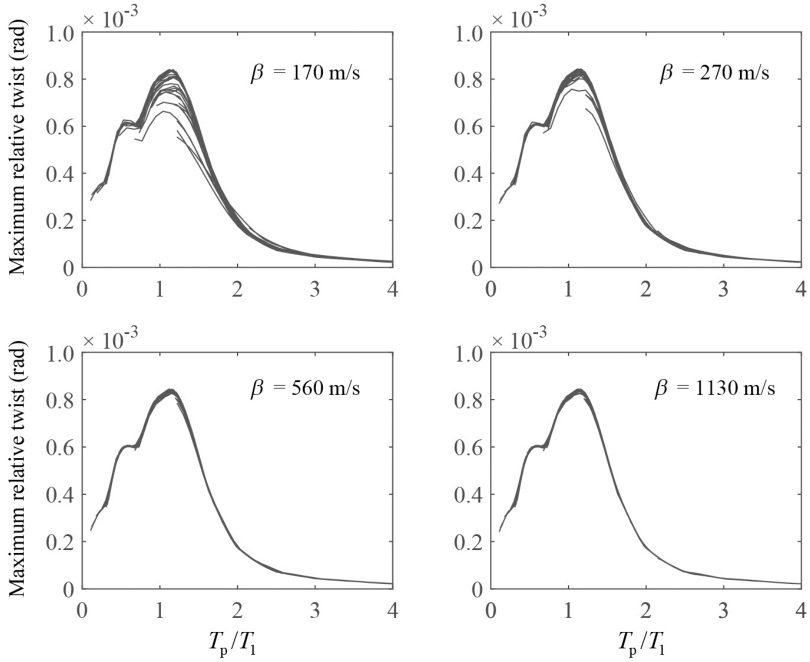

Fig. 4 – Maximum relative twist between top and base of all 40 buildings listed in Table 1 vs. T_{P}/T_1 for $\beta = 170, 270, 560, 1130\ \mathrm{m/s}$. It is assumed that $c_{\mathrm{H}} = 2.0\ \mathrm{km/s}$ and $\gamma = 2.0$.

5. Torsional Response due to Broadband Near-Fault Pulse-Like Ground Motions

5.1 Synthesis of broadband near-fault pulse-like ground motions

Mavroeidis and Papageorgiou [9] proposed a simplified methodology for generating broadband near-fault pulse-like motions adequate for engineering analysis and design. Based on this technique, the coherent (long-period) ground motion component is simulated using the mathematical model presented in Section 3, whereas the incoherent (high-frequency) seismic radiation is synthesized using the specific barrier model (SBM) [21, 22]. This simplified methodology has been applied to both hypothetical and actual earthquakes (e.g. [9, 23]).

In what follows, broadband near-fault pulse-like motions for three hypothetical earthquakes of M_{W} 5.8, 6.4 and 7.0 are simulated, representing moderate, moderate-to-large and large seismic events, respectively. The causative fault is assumed to be a vertical strike-slip fault in an interplate region. Fig. 5 illustrates the fault-station geometry considered herein for the high-frequency ground motion simulations using the SBM. The diameter of the subenvents $2\rho_0$ is 2.1, 4.1, 8.2 km for M_{W} 5.8, 6.4 and 7.0, respectively. According to the calibration of the SBM for interplate regimes [24], the total number of subevents that make up the SBM is typically 15. For consistency and simplicity in our simulations, the 15 subevents are arranged in a 5x3 pattern for all three earthquakes, even though this subevent arrangement may not necessarily be realistic for the M_{W} 7.0 earthquake because of the implied fault width. The station is located in the forward direction with respect to the propagation of rupture and the site characterization is assumed to be NEHRP site class D. The parameters for the simulation of the long-period component using the mathematical model proposed by Mavroeidis and

Papageorgiou [9] are chosen as A = 100 cm/s, γ = 2.0, and $\nu = 90^{\mathrm{o}}$. Based on Eq. (16), the pulse period T_{p} is calculated as 1.0, 2.0 and 4.0 s for M_{W} 5.8, 6.4 and 7.0, respectively.

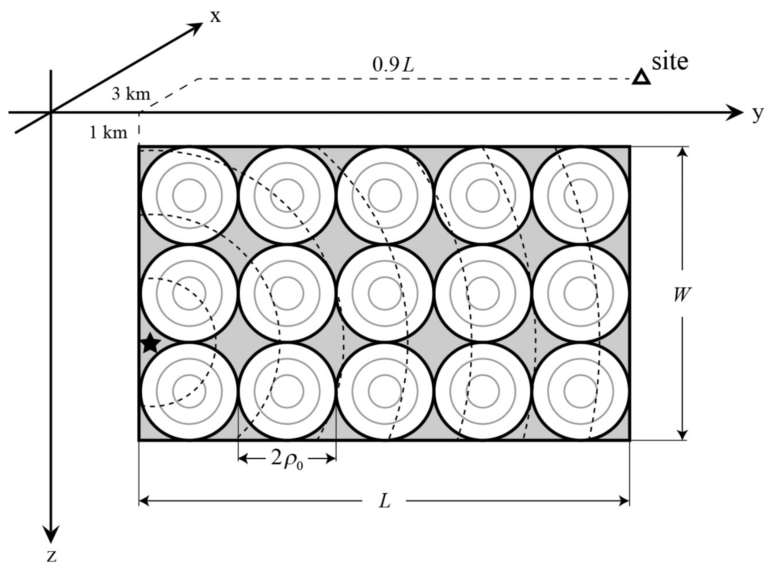

Fig. 5 – Schematic view of the fault-station geometry for the simulation of high-frequency ground motions using the Specific Barrier Model. The dashed lines show the rupture front at successive time instants.

5.2 Results and discussion

Fig. 6 presents the variation of the maximum relative twist as a function of T_1 for all 40 buildings listed in Table 1 due to the hypothetical earthquakes described in Section 5.1. It is assumed that $c_{\mathrm{H}} = 2.0$ km/s and $\gamma = 2.0$, whereas the pulse period T_{P} corresponding to each earthquake is indicated by a dotted vertical line. With reference to Fig. 6, the following observations are made:

- For the M_{W} 5.8, 6.4 and 7.0 earthquakes, the agreement between the values of maximum relative twist due to long-period and broadband ground motions is very good for T_1 > 0.5 s, 1.0 s and 2.5 s, respectively. For smaller values of T_1, the maximum relative twist due to the broadband motion is clearly controlled by the high-frequency component. It should also be noted that the maximum relative twist due to the broadband motion is consistently greater than that of the long-period or high-frequency component.
- The maximum relative twist of short-period buildings (T_1 < 0.5s) appears to be relatively small for all three earthquakes and is controlled by the high-frequency component of ground motion, thus implying that torsional response of short-period buildings due to wave passage is relatively insensitive to near-fault pulse-like motions.
- For both long-period and broadband ground motions, the global peaks of the maximum relative twist are of comparable magnitude and occur for buildings whose torsional period T_1 is close to the pulse period T_{P} of the seismic excitation. This implies that torsional response at resonance is associated with near-fault pulse-like motions. In addition, the maximum relative twist at resonance exceeds 10^{-3} rad, a value that is consistent with the relative twist of a 13-story steel moment-resisting frame building computed by Maison and Ventura [25] and with the upper bound of rotations in structures reported by Trifunac [26].

It should be noted that for symmetric buildings, torsional response may also be caused by ground motion incoherence (associated with the high-frequency component of near-fault ground motions), in addition to the wave passage effects considered herein. Therefore, the actual maximum relative twist of symmetric buildings could potentially be greater than the values obtained in the present study. Moreover, nonlinear soil response, ground failure, and soil liquefaction may induce additional transient and permanent rotations on ground surface near faults, which in turn may further affect the building torsional response [26].

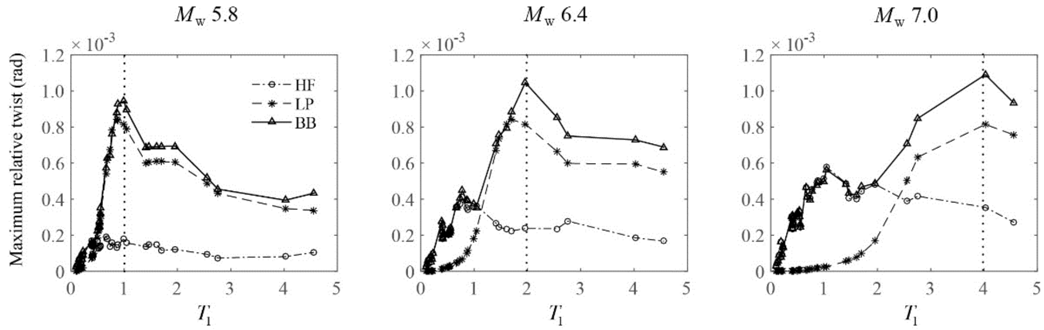

Fig. 6 – Maximum relative twist between top and base of all 40 buildings listed in Table 1 as a function of T_1 due to the high-frequency (HF), long-period (LP) and broadband (BB) ground motions. The pulse period T_P for each earthquake is indicated by a dotted vertical line, whereas $c_H = 2.0$ km/s and $\gamma = 2.0$.

6. Conclusions

The effects of wave passage on the torsional response of symmetric, elastic buildings subjected to near-fault pulse-like ground motions were investigated by considering soil-structure interaction effects and realistic configurations of buildings and soil conditions. The following conclusions are drawn:

- The peak value of the maximum relative twist is attained when the pulse period T_P of the ground excitation approaches the torsional period T_1 of the building, and increases by a factor of ~2 as γ increases from 1 to 3. In addition, the maximum relative twist strongly depends on the wave apparent velocity c_H, rather than the local site conditions. Finally, building parameters such as height and radius have relatively insignificant effect on the relative twist, especially for stiff soil conditions.
- The maximum relative twist of short-period buildings appears to be relatively small and is controlled by the high-frequency component of ground motion, thus implying that torsional response of short-period buildings due to wave passage is relatively insensitive to near-fault pulse-like motions. The maximum relative twist at resonance is controlled by the long-period component of ground motion and exceeds 10^{-3} rad, a value that is consistent with the upper bound of rotations in structures reported in the literature.

As stated by Jennings [27], simplified structural models can be useful in assessing the potential earthquake response of buildings when their detailed properties are not known and in estimating the demands placed on buildings subjected to strong ground motions under the assumption that the building response, although nonlinear, is describable by linear models with appropriate period and equivalent damping. This assumption implies that structural yielding is not excessive and is well distributed over the structure. In addition, simplified structural models have the potential to facilitate the extensive parametric analysis that is frequently required to identify the parameters of the seismic excitation and soil-foundation-structure system that control structural response. Nevertheless, it should be noted that approaches based on simplified structural models are not intended to replace standard practices in the final stages of the design of buildings.

7. Acknowledgements

George P. Mavroeidis and Yenan Cao would like to acknowledge financial support provided by the U.S. National Science Foundation under Grant No. CMMI-1360734.

8. References

[1] Newmark NM (1969): Torsion in symmetrical buildings. *Fourth World Conference on Earthquake Engineering,* Santiago, Chile **3** (2), 19-32.

[2] Luco JE (1976): Torsional response of structures to obliquely incident seismic SH waves. *Earthquake Engineering and Structural Dynamics*, **4** (3), 207-219.

[3] Luco JE (1976): Torsional response of structures for SH waves: the case of hemispherical foundations. *Bulletin of the Seismological Society of America*, **66** (1), 109-123.

[4] De la Llera JC, Chopra AK (1994): Accidental torsion in buildings due to base rotational excitation. *Earthquake Engineering and Structural Dynamics,* **23** (9), 1003-1021.

[5] Juarez M, Aviles J (2008): Effective eccentricity due to the effects of structural asymmetry and wave passage. *Engineering Structures*, **30** (3), 831-844.

[6] Heredia-Zavoni E, Barranco F (1996): Torsion in symmetric structures due to ground-motion spatial variation. *Journal of Engineering Mechanics-ASCE*, **122** (9), 834-843.

[7] Meza-Fajardo KC (2004): Torsional response of structures to impulsive near-fault ground motions. *M.S. Thesis*, State University of New York at Buffalo, Buffalo, NY, USA.

[8] Meza-Fajardo KC, Papageorgiou AS (2004): Torsional response of structures to impulsive near-fault ground motions. presented at the *99th Annual Meeting of the Seismological Society of America*, Palm Springs, CA, USA. [Abstract in *Seismological Research Letters*, **75** (2), 267].

[9] Mavroeidis GP, Papageorgiou AS (2003): A mathematical representation of near-fault ground motions. *Bulletin of the Seismological Society of America,* **93** (3), 1099-1131.

[10] Cao Y, Meza-Fajardo KC, Mavroeidis GP, Papageorgiou AS (2016): Effects of wave passage on torsional response of symmetric buildings subjected to near-fault pulse-like ground motions. *Soil Dynamics and Earthquake Engineering* (in press).

[11] Stewart JP, Seed RB, Fenves GL (1998): Empirical evaluation of inertial soil-structure interaction effects. *Report No. PEER-98/07,* Pacific Earthquake Engineering Research Center, Berkeley, CA, USA.

[12] Stewart JP, Seed RB, Fenves GL (1999): Seismic soil-structure interaction in buildings. II: Empirical findings. *Journal of Geotechnical and Geoenvironmental Engineering-ASCE,* **125** (1), 38-48.

[13] Satake N, Suda K, Arakawa T, Sasaki A, Tamura Y (2003): Damping evaluation using full-scale data of buildings in Japan. *Journal of Structural Engineering-ASCE,* **129** (4), 470-477.

[14] Veletsos AS, Meek JW (1974): Dynamic behavior of building-foundation systems. *Earthquake Engineering and Structural Dynamics,* **3** (2), 121-138.

[15] ASCE (2010): *Minimum Design Loads for Buildings and Other Structures: ASCE Standard 7-10*, American Society of Civil Engineers, Reston, VA, USA.

[16] Mavroeidis GP, Dong G, Papageorgiou AS (2004): Near-fault ground motions, and the response of elastic and inelastic single-degree-of-freedom (SDOF) systems. *Earthquake Engineering and Structural Dynamics,* **33** (9), 1023-1049.

[17] O'Rourke MJ, Bloom MC, Dobry R (1982): Apparent propagation velocity of body waves. *Earthquake Engineering and Structural Dynamics,* **10** (2), 283-294.

[18] Bouchon M, Aki K (1982): Strain, tilt, and rotation associated with strong ground motion in the vicinity of earthquake faults. *Bulletin of the Seismological Society of America,* **72** (5), 1717-1738.

[19] Li B, Al-Bermani FG, Kitipornchai S (1993): Maximum response of asymmetric structures subject to a multicomponent earthquake. *Earthquake Engineering and Structural Dynamics,* **22** (12), 1047-1066.

[20] Aviles J, Suarez M (2006): Natural and accidental torsion in one-storey structures on elastic foundation under non-vertically incident SH-waves. *Earthquake Engineering and Structural Dynamics,* **35** (7), 829-850.

[21] Papageorgiou AS, Aki K (1983): A specific barrier model for the quantitative description of inhomogeneous faulting and the prediction of strong ground motion. I. Description of the model, *Bulletin of the Seismological Society of America*, **73** (3), 693-722.

[22] Papageorgiou AS (2003): The barrier model and strong ground motion. *Pure and Applied Geophysics,* **160** (3), 603-634.

[23] Halldorsson B, Mavroeidis GP, Papageorgiou AS (2011): Near-fault and far-field strong ground-motion simulation for earthquake engineering applications using the specific barrier model. *Journal of Structural Engineering-ASCE,* **137** (3), 433-444.

[24] Halldorsson B, Papageorgiou AS (2005): Calibration of the specific barrier model to earthquakes of different tectonic regions. *Bulletin of the Seismological Society of America,* **95** (4), 1276–1300.

[25] Maison BF, Ventura CE (1991): Dynamic analysis of thirteen-story building. *Journal of Structural Engineering-ASCE,* **117** (12), 3783-3803.

[26] Trifunac MD (2009): Review: Rotations in structural response. *Bulletin of the Seismological Society of America*, **99** (2B), 968-979.

[27] Jennings PC (1997): Earthquake response of tall regular buildings. *Report No. EERL 97-01*, California Institute of Technology, Pasadena, CA, USA.